water

Article

Hydraulic Jump and Energy Dissipation with Sluice Gate

Youngkyu Kim [1], Gyewoon Choi [2], Hyoseon Park [2] and Seongjoon Byeon [3,*]

[1] DOHWA Engineering Co. Ltd., 438, Samseong-ro, Gangnam-gu, Seoul 06178, Korea;
E-Mail: youngkyu@dohwa.co.kr
[2] Department of Civil and Environmental Engineering, Incheon National University,
119, Academy-ro, Yeonsu-gu, Incheon 22012, Korea; E-Mails: gyewoon@incheon.ac.kr (G.C.);
kokomanara84@naver.com (H.P.)
[3] International Center for Urban Water Hydroinformatics Research & Innovation, 169, Gaetbeol-ro,
Yeonsu-gu, Incheon 21999, Korea

* Author to whom correspondence should be addressed; E-Mail: seongjune@paran.com;
Tel.: +82-32-835-4760; Fax: +82-32-851-5730.

Abstract: Movable weirs have been developed to address the weaknesses of conventional fixed weirs. However, the structures for riverbed protection downstream of movable weirs are designed using the criteria of fixed weirs in most cases, and these applications cause problems, such as scour and deformation of structures, due to misunderstanding the difference between different types of structures. In this study, a hydraulic experiment was conducted to examine weir type-specific hydraulic phenomena, compare hydraulic jumps and downstream flow characteristics according to different weir types, and analyze hydraulic characteristics, such as changes in water levels, velocities and energy. Additionally, to control the flow generated by a sluice gate, energy dissipators were examined herein for their effectiveness in relation to different installation locations and heights. As a result, it was found that although sluice gates generated hydraulic jumps similar to those of fixed weirs, their downstream supercritical flow increased to eventually elongate the overall hydraulic jumps. In energy dissipator installation, installation heights were found to be sensitive to energy dissipation. The most effective energy dissipator height was 10% of the downstream free surface water depth in this experiment. Based on these findings, it seems desirable to use energy dissipators to reduce energy, as such dissipators were found to be effective in reducing hydraulic jumps and protecting the riverbed under sluice gates.

1. Introduction

Weirs are structures installed across rivers in order to raise water levels and prevent backward water flow for efficient water intake and waterway use. Previously, the concrete gravity dam (CGD) was a frequently utilied weir type for water overflow weirs. The CGD slows water inflow from upstream before reaching a weir and allows it to flow over the weir. Thus, the flow velocity falls and inflowing silt is deposited. In this manner, the water storage capacity decreases and weirs lose their initial effectiveness. Therefore, efforts have been made to develop various movable weirs to reduce such sedimentation processes and fulfil their original purposes for the long term. Concerning movable weirs, there is a turning gate-type movable weir, which turns a weir to discharge silt sedimentation, and a sluice gate-type weir, which lifts a weir to do so [1–3].

With weirs in place, upstream water levels move up to ease water intake and waterway use. However, the hydraulic jumps caused by weirs increase in terms of their head drop and velocity, thus causing bed scour and other damage to hydraulic structures. As methods to prevent such scour, aprons and bed protection have been installed in the lower parts of weirs as energy dissipators for hydraulic jump control.

In order to protect hydraulic structures and rivers from the energy generated by hydraulic structures, the United States Department of the Interior Bureau of Reclamation (USBR) established the Engineering Monograph No. 25 in 1964 for the energy dissipators of hydraulic structures and energy reduction. In the monograph, the hydraulic jump phenomenon was divided into four forms dependent upon Froude numbers. Based on various other hydraulic experiment findings, it suggested 10 different types of stilling basins and energy dissipators appropriate for each discharge type and spillway type. The monograph has continuously upgraded its improvement measures since then [4].

Concerning broad-crested weirs and flows with Froude numbers between 2.5 and 4.5, which accompany huge hydraulic changes, Bhowmik (1971) combined energy dissipators (baffle blocks and end stills), presented 11 types of energy dissipators and examined each of their energy dissipation performances [5]. Rajaratnam and MacDougall (1983) reported that partially submerged orifice flow showed approximately a 50% reduction in scour depth compared with completely submerged orifice flow, whereas its scour length increased by 25%–50% [6]. Yoon *et al.* (1995) analyzed the scour hole characteristics in a free-falling jet generated by drop structure dependent upon the existence of mound in their weir experiment. They found that if a density Froude number increased, not only the equilibrium scour depth, but also the mound heights moved up [7]. Hoffmans and Verheij (1997) utilized the ratio of flow velocity at the weir discharge jump to the post-hydraulic jump velocity to suggest the maximum scour depth. The researchers proposed that the maximum scour depth appeared at a distance amounting to two times as far as the maximum scour depth from the scour start. They also suggested that scour-caused riverbed variation could be observed up to 5–7 times longer than the maximum scour length and 3–4 times wider than the maximum scour depth [8]. Concerning weir flow, Fahlbusch (2003) presented an equation to calculate scour depths according to the different velocities and drop angles of

water-overflowing weirs. He reported that scour depths decreased as downstream water levels increased [9].

Noshi (1999) measured velocity changes at the river bottom to assess the energy dissipation of end sills in spillway flow. The researcher analyzed downstream hydraulic jump lengths and suggested they were approximately 2.3 times as long as the downstream water level [10]. Verma and Goel (2003) performed a hydraulic experiment and proposed a new shape of energy dissipator (wedge-shaped block) as a way to reduce the jet flow discharged through culverts. The researchers also stated that tooth-formed energy dissipators were more useful than the conventional rectangular dissipators in energy dissipation [11]. Jeong (2011), in his hydraulic model experiment, proposed a method to calculate apron length dependent upon upstream/downstream water levels with movable weirs and weirs fixed in place [12].

Many studies have focused on measuring hydraulic jump lengths and the energy differences between the upstream and downstream of weirs in order to determine the length of aprons or shorten hydraulic jumps through energy dissipation. However, an insufficient amount of studies on movable weirs have been developed more recently compared with studies on fixed weirs. Therefore, structures for river-bed protection, which are applied in several river maintenance projects, have occasionally been determined through the estimation of weighted values without factoring in the characteristics of different movable weir types. Additionally, this study discusses the energy dissipator in particular as one of major structures for riverbed protection. Therefore, this study examined the hydraulic phenomena generated by the installation of a sluice gate-type movable weir and performed a hydraulic experiment to review and propose an effective energy dissipation method. Through the experimental study and analysis, hydraulic characteristics, such as the length of the hydraulic jump and the installation of an energy dissipator, have been formulated for applications. In addition, this study sought to describe the design criteria of energy dissipators for riverbed protection in movable weirs, which were inadequately reflected in the present design standards.

2. Methodology and Experiment

To control hydraulic jump and enhance hydraulic jump efficiency, sills such as sharp-crested weirs, broad-crested weirs or end sills at the bottoms of waterways are frequently used. The force acting upon such a sill in the hydraulic jump rapidly decreases to the minimum as the end point of roller at downstream of the hydraulic jump moves upward at a point where it almost overflows a sill. This impact of sills can make the length of the scour risk zone shorter than a normal hydraulic jump phenomenon. Then, as the hydraulic jump becomes shorter and moves further upstream, the force upon a sill gradually increases to reach a certain level. Since such a rapidly varying flow is characterized as having an uneven velocity distribution, the changes in force upon a sill seem to be because of the changes in velocity distribution occurring between the starting points of the hydraulic jump to its end point. Consequently, in a cross-section with unequal velocities, the momentum surges greatly. Theoretically, hydraulic jump controlled by sills can be interpreted using the momentum theory. However, in the absence of a precise theory of velocity distribution, an accurate quantification can hardly be made by just relying on theoretic interpretation. An experiment for simulating the behavior of a sluice gate and an associated hydraulic jump experiment have been carried out in different conditions to enable an investigation of the

characteristics of hydraulic jump, and to analyze energy dissipation, the physical experiment collects data that are afterwards used to define relations, which are used as guidelines for design operations.

2.1. Experiment Equipment and Method

The open-channel system used in this experiment is a channel installed in a hydraulic experiment lab of Incheon University, Korea.

The straight-line channel is 11.0 m in total length, 0.7 m in width, and 0.8 m in height and has reinforced glass walls for flow observation. It has three distribution plates at the inlet to induce steady-state inflow. Although inflow passes through the distribution plates to become steady, in order to minimize the inlet contraction effect, a fixed weir and sluice gate weir were installed at points 2.0 m away from the inlet. Vertical grooves were made on the left and right sides of the channel to install weirs at the same height and adjust movable weir heights. Since it is occasionally hard to measure the variation of flow surface created by the hydraulic jump, besides using a velocimetry and a point gauge, piezometers were installed on the bottom of the channel to monitor water pressure to estimate hydraulic characteristics. The installed piezometers were attached to the walls for the purpose of observation.

In order to install and adjust the weirs and piezometers, an acrylic-plate channel was made by distancing each 0.10 m inward from the left side, right side and bottom. Figure 1 shows the channel cross section. The piezometers were installed in three rows at 0.08 m intervals toward the channel center on the left side from a point approximately 0.20 m away from the weir installation. The installation intervals were 10 cm long, and a total of 60 piezometers were installed. The maximum water supply of the installed pump was 0.056 m^3/s. However, given the channel size and to ensure constant flow maintenance, 0.026 m^3/s was supplied as the maximum. The variation of the pressure head caused by the installation of the weir could be observed through the piezometers. In order to measure detailed hydraulic characteristics, the 2-D velocity meter (VP1200, KENEK Corp., Tokyo, Japan), which uses very thin sensor needle, was used to minimize flow interference.

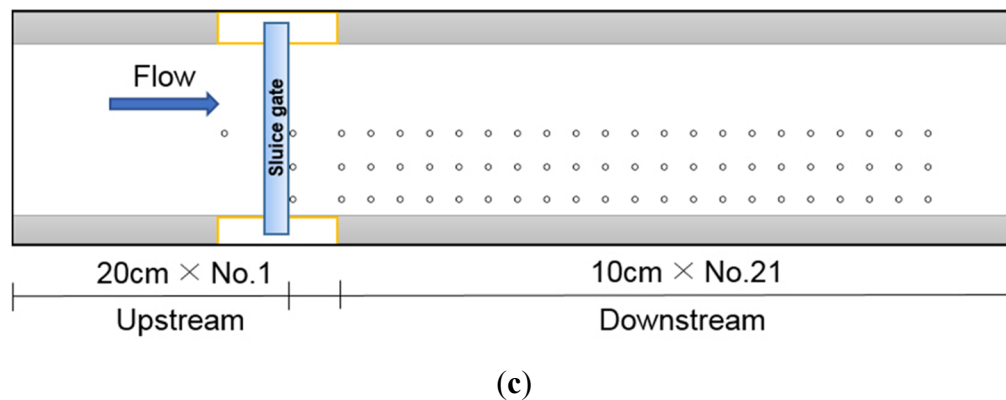(a)   (b)

Figure 1. *Cont.*

(**c**)
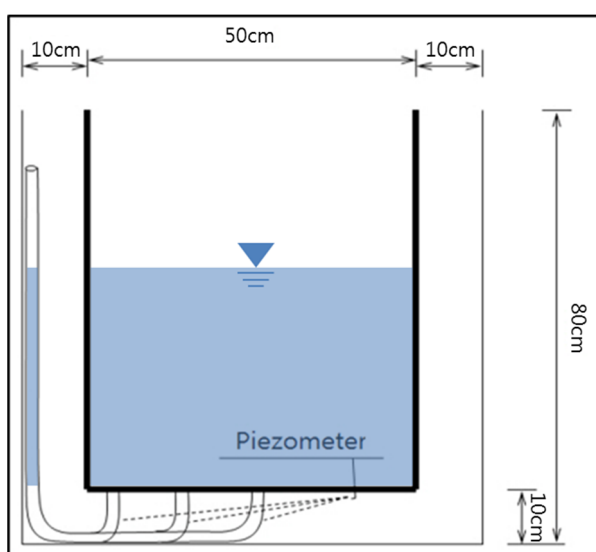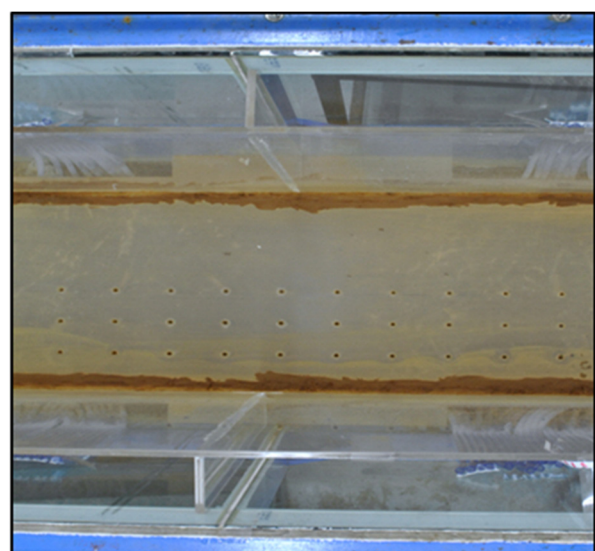
Figure 1. Structure diagram of channel. (**a**) Cross-sectional view with piezometer; (**b**) Floor plan showing the piezometer hole in the channel; and (**c**) weir and the channel.

As the fixed weir and sluice gate-type weir have different shapes, the centers of the two different weirs were made sure to be in the same position for installation consistency.

The fixed weir was 0.1 m in height, 0.05 m in upper width, 0.11 m in lower width and had a 1:0.7 ratio for the overflow slope. The sluice gate-type weir was 0.3 m in height and 0.01 m in thickness. Figure 2 shows the overflow-type weir.
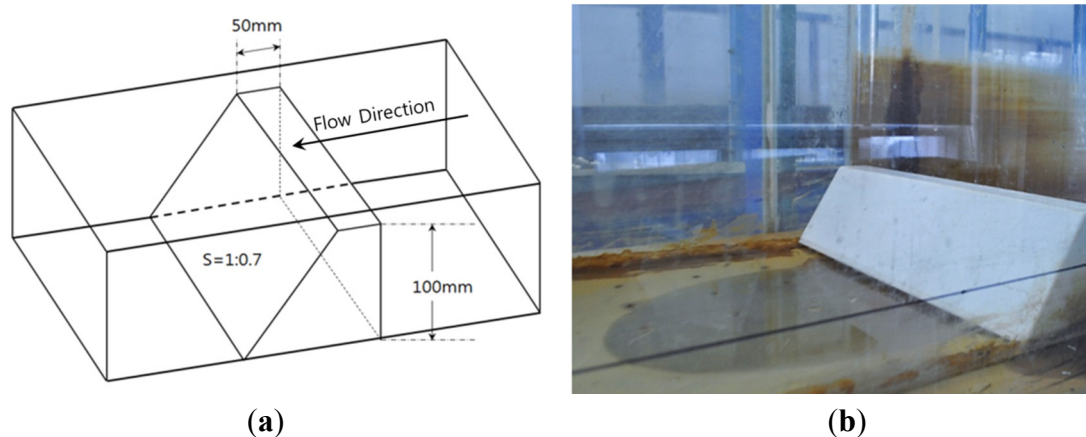

(**a**)   (**b**)

Figure 2. Overflow-type fixed weir (**a**) plan of fixed weir installation; (**b**) photo of weir installed in the channel.

As the sluice gate movable weir changes its openness heights, the experiment devices should be structured to accept such changes. Therefore, after fixing the weir, grooves of 0.01 m width and 0.005 m depth were made on the left and right walls of the channel for the free height change. To prevent possible leakage through the weir bottom when the sluice gate is completely closed, the same 0.01 m wide and 0.005 m deep grooves were made and the back wall of the fixed weir was elongated by 0.005 m to fit in, as shown in Figure 3.

As mentioned in the introduction on the effectiveness of energy dissipators in the use of a conventional fixed weir, it was found that tooth-formed blocks were more effective than total cross-section installation. However, as the present study does not aim to examine certain targeted rivers, but rather to produce experiment results based on unit width, the authors tried to install the whole widths of the experiment channel throughout, as shown in Figure 4.
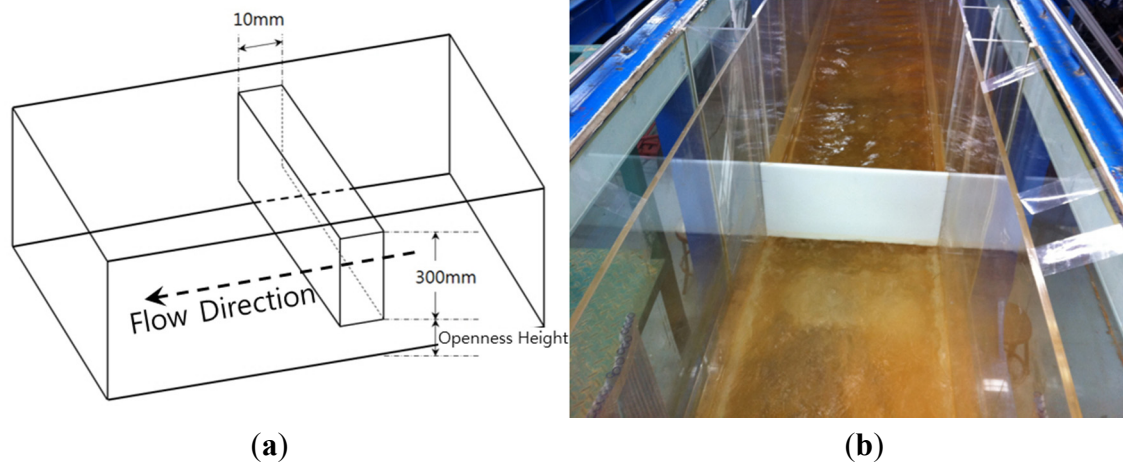
Figure 3. Sluice gate-type movable weir (**a**) plan of sluice gate installation; (**b**) photo of sluice gate installed in the channel.
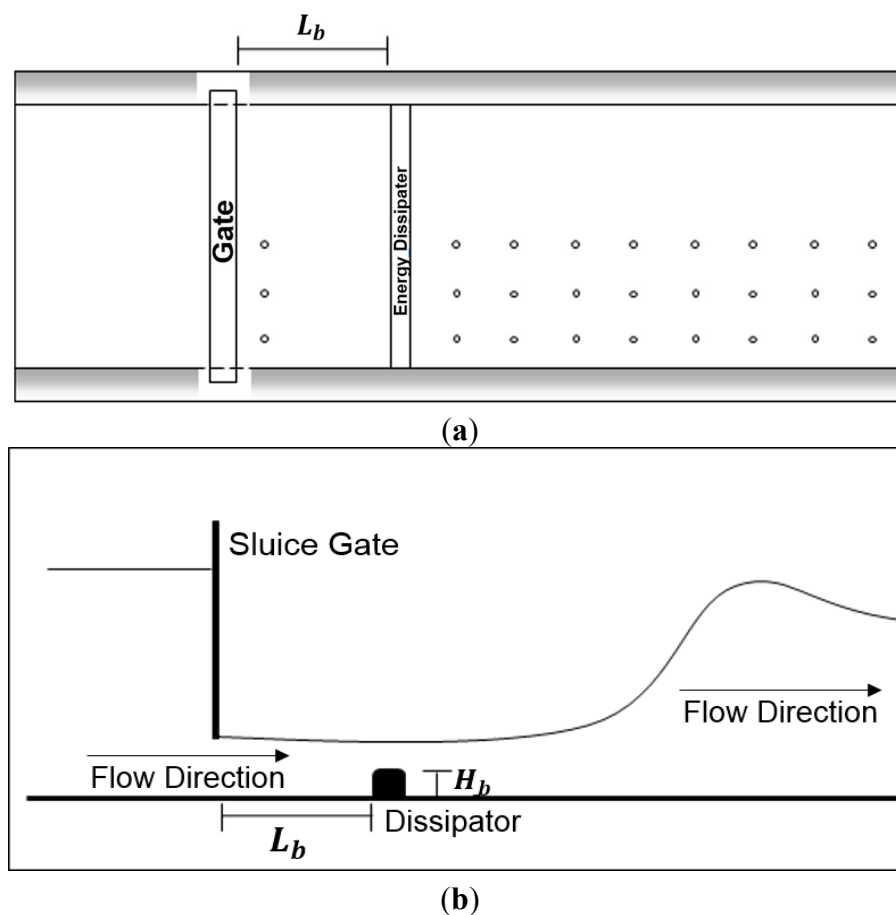

Figure 4. Installation diagram of energy dissipator: (**a**) Horizontal plan; (**b**) Longitudinal plan.

The dissipators used herein were 500 mm long to fit into the whole width of the channel. The width of the dissipators was set at 10% of the average downstream water depth measured in a preliminary experiment. The heights of the dissipators were set at 5%, 10% and 15% of the average downstream water depth in order to compare diverse cases, as in Table 1, which shows the height of the model.

Table 1. Height of energy dissipator.

Mean Downstream Depth	Height of Energy Dissipator (Hb)		
	5%	10%	15%
100 mm	5 mm	10 mm	15 mm

In this research, different flow patterns were investigated according to weir installation types and hydraulic jump starting points and their lengths were measured. To compare the flow patterns of fixed weir and sluice gate-type movable weirs, the constant upstream water level of the fixed weir was measured and applied to the movable weir case, since the fixed-weir upstream water levels were constant at each different flow rate. In order to keep the upstream water level constant in the movable weir case, its opening rate was adjusted.

In the movable weir experiment herein, the openness height was changed to produce Froude numbers to measure and compare the velocities and water levels at the discharge point from the gate. The measurement points were marked on the upper part of the experiment channel to ensure the measurement was performed at the same point. The main measurement points are shown in Figure 5.
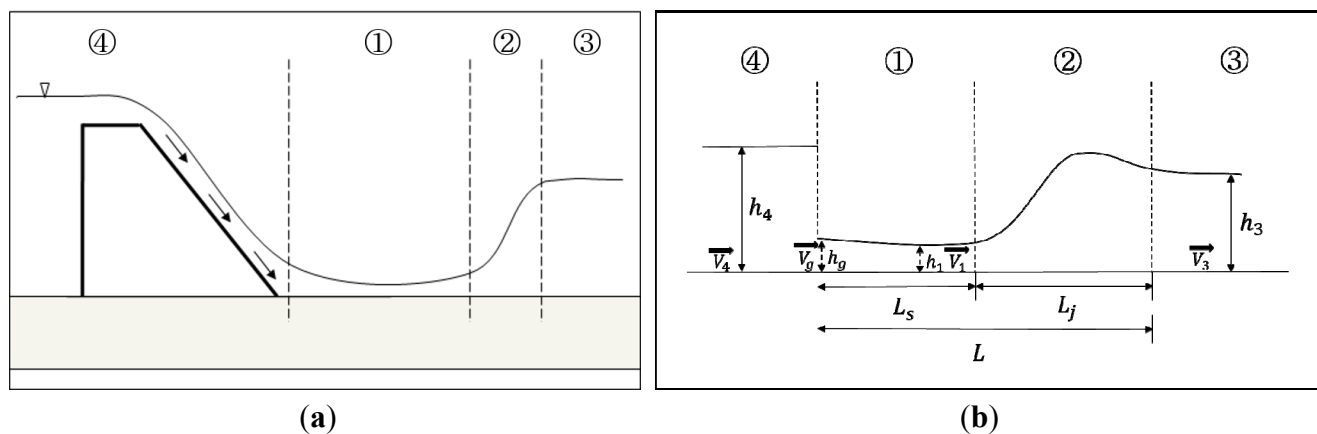

(a)   **(b)**

Figure 5. Measurement regions of fixed weir and movable weir (**a**) Measurement point of fixed weir and (**b**) Measurement point of movable weir.

Figure 5 shows the following region-specific characteristics:

(1) Region 1: A supercritical flow region formed when water is discharged by the sluice gate-type movable weir. The flow conditions in Region 1 and associated Froude number are used to describe each experiment.
(2) Region 2: Hydraulic jumps appear in this region in the discharged water flow of the sluice gate-type movable weir. The hydraulic jump lengths are calculated from the existing equations.
(3) Region 3: The discharged flow stabilizes after the hydraulic jumps in this region to show a similar flow to that of the fixed weirs.
(4) Region 4: The upstream domain of the weir region.

Each region was separated based on distinguished flow characteristics. Region 1 with supercritical flow, especially, showed different patterns from those of the fixed weir dependent upon flow rates. To avoid the effect of the channel walls, the central part of the channel was measured in this experiment.

As fixed-weir flow and movable-weir flow are slightly different, the measurement locations were determined as shown in Figure 5 to ensure identical factors were compared.

The supercritical flow region was recognized as Region 1; the hydraulic jump region as Region 2; and the post-hydraulic jump flow identical to that of the weir-free open channel as Region 3. Additionally, the upstream weir section elevated by the weir installation was recognized as Region 4. To ensure the same upstream conditions, the movable weir openness heights were adjusted to meet the equal water depth.

This study examined the flow characteristics variation according to sluice gate-type movable weir operation and downstream water level conditions as well as hydraulic jump, changes in their lengths and energy variation. To examine flow changes dependent upon the openness height of the movable weir, the movable weir openness height was changed to help generate diversified flow patterns in the channel after passing through the sluice gate. That is, the water flow moving through the sluice gate movable weir showed a similar pattern to the flow through the orifice. Orifice flow was also diversified dependent upon the submerged level, including the completely submerged orifice and partially submerged orifice. Therefore, the opening rate of the sluice gate-type movable weir was determined to show diverse patterns in this experiment. For each flow, the minimum movable weir openness height was determined by opening the movable weir until supercritical flow and all upstream flows appeared in the experiment channel. The openness height of sluice gate was then determined to make a similar condition to the fixed weir under the same flow rate, as shown in Table 2.

Table 2. Condition of flow rate and openness height of sluice gate.

Flow Rate (m³/s/m)	Openness Height (m)	Remarks
0.036	0.026	There are additional openness heights (m) of extended cases for Chapter 5 (Energy dissipation) (0.036, 0.039, 0.042 and 0.045)
0.044	0.036	
0.052	0.036	

2.2. Changes in Energy after Weir Installation

Regarding the energy loss other than the water depth fluctuation before and after the hydraulic jump, ΔE is the amount of pre-hydraulic jump energy, E_1, less than the post-hydraulic jump energy, E_2,

$$\Delta E = E_1 - E_2 = \left(h_1 + \frac{V_1^2}{2g}\right) - \left(h_2 + \frac{V_2^2}{2g}\right) = (h_1 - h_2)\left[\frac{q^2}{2g}\frac{h_2 + h_1}{h_1^2 h_2^2} - 1\right] \quad (1)$$

where h_1 (m) is a water depth before the hydraulic jump, h_2 (m) is a water depth after the hydraulic jump as a conjugate depth, V_1 and V_2 (m/s) are the flow velocity of the pre/post-hydraulic jump, respectively, and q (m³/s/m) is a unit of water flow rate in the channel.

However, based on the momentum equation:

$$\frac{1}{2}(h_1 + h_2) = \frac{q^2}{gh_1 h_2} \quad (2)$$

If Equation (3) is substituted into Equation (2),

$$\Delta E = \frac{(h_2 - h_1)^3}{4h_1 h_2} \quad (3)$$

The hydraulic jump-caused energy loss can be calculated simply with the pre/post-hydraulic jump water depths. The specific forces for the pre/post-hydraulic jump water depths h_1 and h_2 are the same. However, the specific energy curve shows that the specific energy of h_2, E_2, is smaller than the specific energy of h_1, E_1, by ΔE. This is the energy loss due to the hydraulic jump.

If both sides of Equation (4) are divided by h_1 and expressed by the post-hydraulic jump Froude Numbers as Fr_1,

$$\frac{\Delta E}{h_1} = \frac{\left(-3 + \sqrt{1 + 8Fr_1^2}\right)^3}{16\left(-1 + \sqrt{1 + 8Fr_1^2}\right)} \tag{4}$$

Equation (5) can be expressed solely by the function of the Froude Number Fr_1 regarding the pre-hydraulic jump water level and hydraulic jump-caused energy loss.

The pre-hydraulic jump specific energy, E_1, is,

$$E_1 = h_1 + \frac{V^2}{2g} = h_1 + \frac{q^2}{2gh_1^2} \tag{5}$$

If both sides of Equation (6) are divided by h_1,

$$\frac{E_1}{h_1} = 1 + \frac{q^2}{2gh_1^3} = 1 + \frac{1}{2} Fr_1^2 \tag{6}$$

If Equation (5) is divided by Equation (7),

$$\frac{\Delta E}{E_1} = \frac{\left(-3 + \sqrt{1 + 8Fr_1^2}\right)^3}{8\left(-1 + \sqrt{1 + 8Fr_1^2}\right)\left(2 + Fr_1^2\right)} \tag{7}$$

The $\Delta E/E_1$ expressed by Equation (8) is called a relative loss.

$$\frac{E_2}{E_1} = 1 - \frac{\Delta E}{E_1} = \frac{(1 + 8Fr_1^2)^{3/2} - 4Fr_1^2 + 1}{8Fr_1^2(2 + Fr_1^2)} \tag{8}$$

In Equation (9), the ratio of pre/post-hydraulic jump specific energies (E_2/E_1) is called the hydraulic jump efficiency. The hydraulic jump height refers to the difference between the pre/post-hydraulic jump water depths or $\Delta h = h_2 - h_1$, and the following relation formula can be proven.

$$\frac{\Delta h}{E_1} = \frac{h_2}{E_1} - \frac{h_1}{E_1} = \frac{-3 + \sqrt{1 + 8Fr_1^2}}{2 + Fr_1^2} \tag{9}$$

where $\Delta h/E_1$, h_1/E_1 and h_2/E_1 are called the relative hydraulic jump heights, pre-hydraulic jump and post-hydraulic jump relative water depth, respectively.

3. Results

3.1. Flow Changed with Overflow-Type Fixed Weir and Sluice Gate-Type Mobile Weir

The hydraulic flow of the fixed weir and the sluice gate-type movable weir installation described in the previous sections were compared and analyzed. The fixed and movable weir flow patterns were analyzed while maintaining the flow and water level at the same levels—the weir upstream conditions. Table 3 shows the upstream conditions of the experiment.

Table 3. Experiment conditions.

Flow Rate (m³/s/m)	q (m³/s/m)	v_4 (m/s)	h_4 (m)	Fr_4
	0.036	0.19	0.19	0.14
Fixed weir	0.044	0.20	0.22	0.16
	0.052	0.21	0.25	0.19
	0.036	0.19	0.19	0.14
Sluice gate	0.044	0.20	0.22	0.16
	0.052	0.20	0.26	0.19

As shown in the table, the experiment flow flowed in, and then the movable weir height was adjusted to create equal upstream water levels and upstream conditions for both types of weirs. The hydraulic jump lengths were divided by the water depth h_1 in the supercritical flow region before the hydraulic jump phenomenon occurred to generalize the hydraulic jump lengths. Table 4 shows the hydraulic jump length per unit flow and Froude number measured at h_1, and Figure 6 shows the hydraulic jump lengths per unit flow.

Table 4. Hydraulic jump lengths and Froude number at each type of weir.

Q (m³/s/m)	Fixed Weir			Sluice Gate			$\Delta L_j/h_1$
	h_1 (m)	L_j/h_1	Fr	h_1	L_j/h_1	Fr	
0.036	0.02	55.30	3.36	0.02	90.55	3.16	35.25 (64%)
0.044	0.02	78.26	3.56	0.03	105.26	3.43	27.00 (35%)
0.052	0.03	91.25	3.89	0.03	112.32	3.74	21.07 (23%)
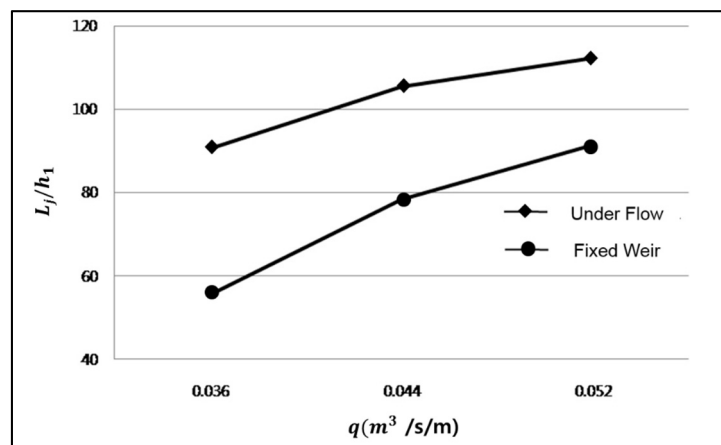
Figure 6. Hydraulic jump lengths occurring per unit flow rate.

The dimensionless value of the hydraulic jump (L_j/h_1) of the fixed weir at a flow of 0.036 m³/s/m was 55.30, and that of the movable weir was 90.55. When the flow was 0.044 m³/s/m, the dimensionless value of the fixed weir was 78.26 and that of the movable weir was 105.26. When the flow was 0.052 m³/s/m, the dimensionless value of the fixed weir was 91.25, and that of the sluice gate-type movable weir was 112.32. The lower the flow, the more the gap between the two values increased, and

the maximum increase of 64% was recorded when the flow was 0.036 m³/s/m under the sluice gate-type movable weir.

The differences in hydraulic jump lengths represented by the dimensionless expression as $(\Delta L_j/h_1)$ were found to be 35.2, 27.0 and 21.1 for each flow, showing that the lower the flow, the longer the difference of hydraulic jump lengths of fixed weir and movable weir. Compared with the fixed weir, in the movable weir, the hydraulic jump length increase rate ranged from 64% to 23% in each case.

Figure 7 shows hydraulic jump length as the distance when the flow is stabilized according to the Froude numbers of the discharge point.

Both the fixed weir and movable weir were found to have longer distances of hydraulic jump as the Froude numbers became higher. When the Froude number was 3.7, the movable weir L_j/h_1 was 112.32, approximately two times larger than the fixed weir L_j/h_1, 55. The sluice gate-type movable weir was found to have a longer hydraulic jump length than that of the fixed weir because the fixed weir diverted flow to dissipate the energy at the bottom. Thus, sluice gate-type movable weirs may need a flow energy dissipation facility in a place where the fixed weirs do not need one.
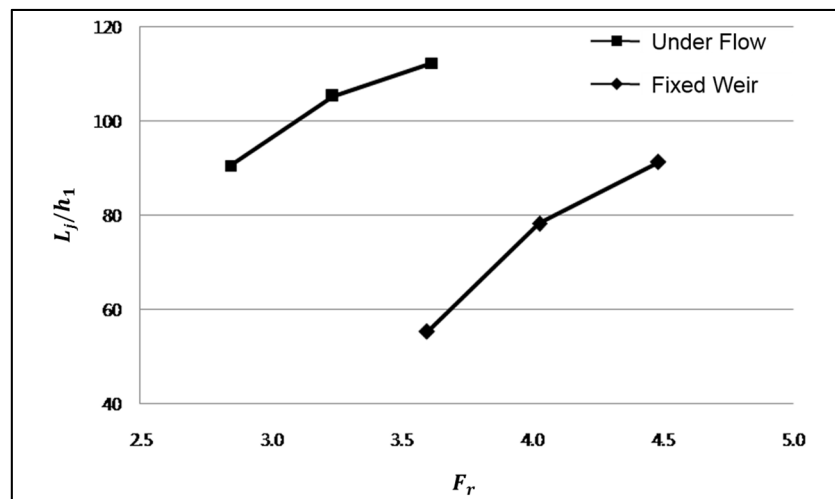

Figure 7. Hydraulic jump lengths occurring according to Froude numbers.

3.2. Flow Changes According to Different Openness Heights

In order to examine flow changes according to different openness heights of the sluice gate-type movable weir, the openness height of the sluice gate-type movable weir was changed to generate diverse flow patterns after passing through the sluice gate. That is, the post-sluice gate flow showed a similar pattern to that of the flow through orifice. Additionally, the orifice flow was further divided into the completely submerged orifice and partially submerged orifice. Therefore, the opening rate of the sluice gate of the movable weir was set to observe diverse flow patterns herein.

The minimum movable weir openness height was determined by opening the movable weir until supercritical flow and all of the upstream flows were observed in the experiment channel. The openness height was then increased by 3 mm each time to analyze the flow changes.

In the movable weir, the discharged flow showed a high velocity and low water depth to create supercritical flow with Froude numbers exceeding 1.0. However, as the movable weir height increased and the discharged cross-sectional area of flow grew larger, the velocity decreased despite the same

amount of inflow. As the movable weir openness height moved up, the Froude numbers became smaller at the discharge point, and the supercritical flow and hydraulic jump lengths were reduced.

If the flow increased, the post-hydraulic jump water levels moved up. Such water levels were found to be higher at 0.044 m³/s/m than at 0.036 m³/s/m by 20 mm or more. Higher water levels affected the upstream flow, thus reducing hydraulic jump sizes as well as hydraulic jump lengths to a considerable extent. In particular, if a movable weir was high, the hydraulic jump was shortened. In this case, the water level of the outlet area grew higher, the velocity decreased and hydraulic jump did not occur.

Figure 8 shows the conjugate water depths according to the Froude numbers of the outlet area. Conjugate depth refers to the ratio of the water depth of the supercritical flow region to the water depth of the post-hydraulic jump stabilization section. Depending on the sluice gate openness height, conjugate water depth values vary.
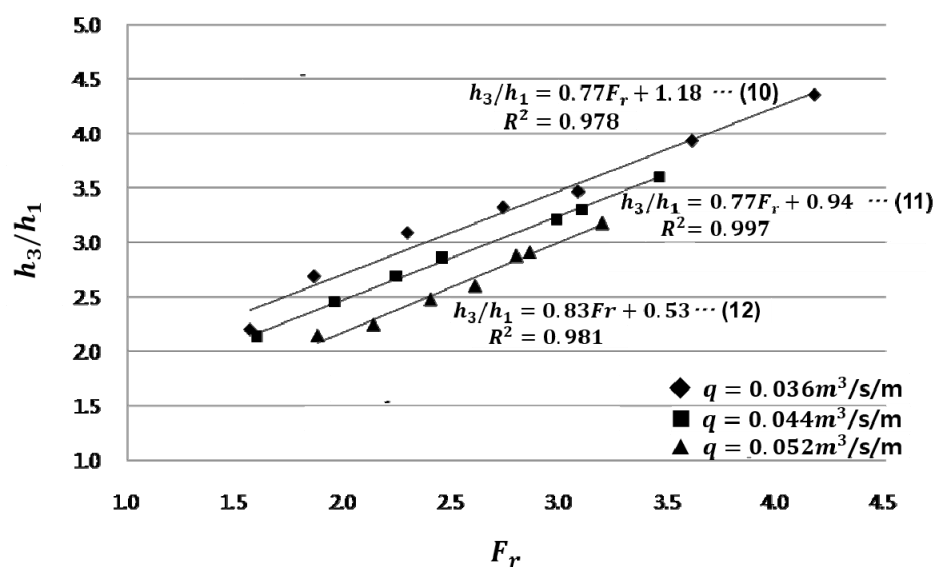

Figure 8. Conjugate water depth according to experiment flow rates and Froude number.

As shown in Figure 8, the Froude numbers of the outlet area show a proportional relation with conjugate depth. That is, due to the same amount of flow inflows, the post-hydraulic jump water depth (h_3) is the same. However, the discharge water depth reduction in the case of discharge results in conjugate depth elevation and Froude number increases. Therefore, the conjugate depth and Froude numbers have a proportional relation. However, if water is discharged while keeping the Froude number the same, the flow rate increases to also increase the post-hydraulic water level as well as the corresponding conjugate depth, as shown in Figure 8.

4. Hydraulic Jump Length Calculation Equation

The existing formula for hydraulic jump length presents the relationship between hydraulic jump length and supercritical flow water depth according to Froude numbers. In this study, to compare the existing formula regarding the net hydraulic jump length (L_j) with the measurement results, Figure 9 was provided. The hydraulic jump length (L_s) was separately reviewed herein.
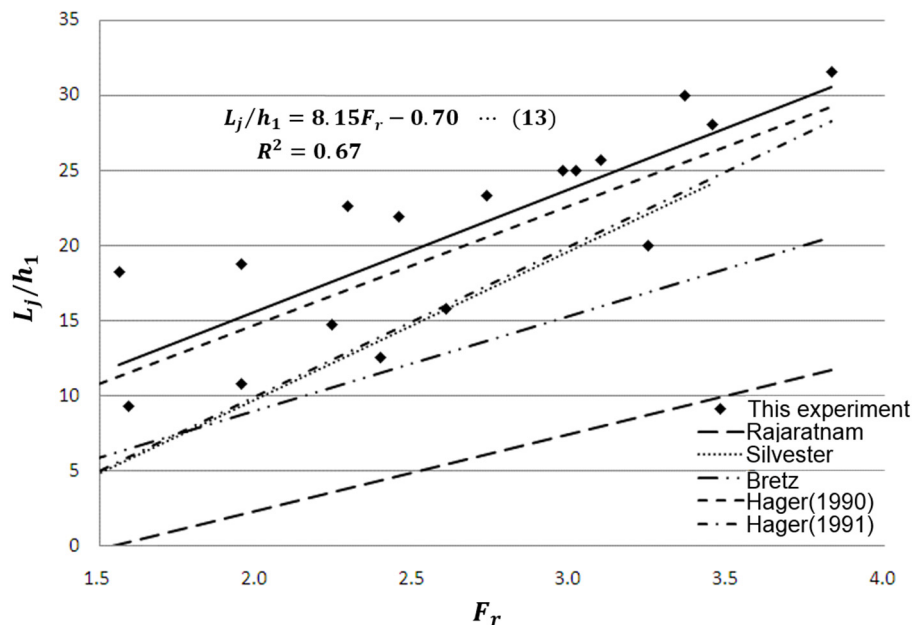
Figure 9. Measurements and comparison with previous studies.

Many researchers have suggested formulas for hydraulic jump length, such as that presented by Silvester [13]. Rajaratnam's Equation and Bretz's Equation suggest that hydraulic jump length has a linear relationship with Froude numbers. Silvester's Equation is presented in an exponential function, although it is similar to Rajaratnam and Bretz's Equations [14]. Hager (1992) used a trigonometrical function to structure a relation function along with a conversion formula [15]. In the present study, Froude numbers within the range of 1.5–4.0 are considered, and they represent the lowest hydraulic jump length calculated by Rajaratnam's Equation, while representing the highest value calculated by Hager's equation, similar to the present research results. Based on the research results, a regression equation was structured and presented in Equation (13) as follows:

$$\frac{L_j}{h_1} = 8.15 \, Fr - 0.70 \tag{13}$$

The root mean square error (R^2) from the regression equation was calculated as 0.67. It seemed that this was because the hydraulic jump lengths were changed by the effects of the left and right walls.

Many other studies have empirical formulas designed through experiments on fixed weirs. Compared with the research results, all of the outcomes tend to be proportional to Froude numbers, showing the similarity of the presented results. The difference between the Equation (13) and measurement is thought to be because of subjective aspects of the experiment, such as changes in the experimental conditions and errors. Therefore it is possible to estimate there is no huge difference in hydraulic jump lengths between the movable weir and fixed weir in terms of using the dependent variable of Froude numbers in supercritical condition, and the result is in direct proportion to the Froude numbers. However, the hydraulic jump flow of the fixed weir and movable weir shows a huge gap due to the supercritical flow length. In the same flow and upstream conditions, the fixed weir and movable weir show a remarkable difference in hydraulic jump. However, concerning the hydraulic jump phenomenon generated by the difference between pre/post-hydraulic jump energy, since the fixed weir and movable weir have the same amount of energy dissipated by the hydraulic jump though their discharge types

being different, their hydraulic jump lengths are deemed similar. However, as shown in the experiment results, there was a big difference in the distance from the weir to the end of hydraulic jump. Therefore, the supercritical flow length excluding the hydraulic jump length is separately reviewed herein.

The distance to the hydraulic jump start point (L_s) was reviewed by the ratio of the distance from the movable weir to the post-hydraulic jump flow stabilized as the open-channel flow (L). By comparing it with Froude numbers, the relationship between the two factors was expressed in a diagram, as shown in Figure 10.

A linear regression equation was produced as in Equation (14):

$$\frac{L_s}{L} = 0.25\,Fr - 0.18 \tag{14}$$

The ratio of hydraulic jump length (L_s/L) was found to be proportional to the Froude numbers, and the deviation (R^2) was 0.86, representing a close relationship with the proposed regression equation.

As the distance from the movable weir to the hydraulic jump end point can be expressed as the sum of the distance to the hydraulic jump start and hydraulic jump length, the Equation (15) is presented as follows:

$$\frac{L_j}{L_s} + 1 = \frac{1}{0.25Fr - 0.18} \tag{15}$$

The distance to the hydraulic jump starting point (L_s) can be expressed by a relation equation between a Froude number and hydraulic jump length (L_j). In Equation (16), L_s is expressed as an equation regarding L_j, as follows:

$$L_s = \left(\frac{1}{1.18 - 0.25Fr} - 1\right) L_j \tag{16}$$

The equation described above can be used to estimate hydraulic jump lengths in hydraulic jump phenomena frequently occurring in the conventional fixed weirs of a dam spillway as well as sluice gate-type movable weir for designing aprons and bed protections.
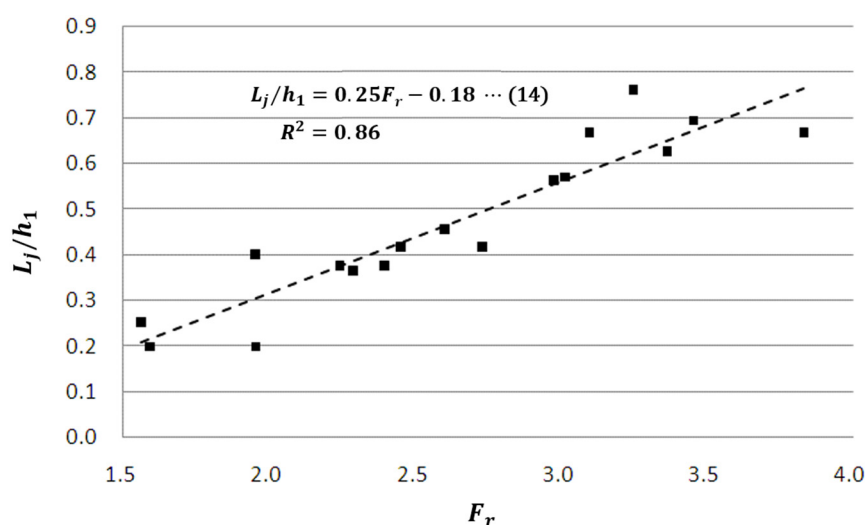

Figure 10. Compared with Froude numbers, relationship between L_s and L.

5. Energy Reduction in Energy Dissipator

5.1. Energy Reduction According to Dissipator Installation Heights

In this study, energy dissipators were installed at heights of 5%, 10% and 15% of downstream water depth to examine energy dissipation dependent upon installation heights with a flow rate specified as 0.052 m^3/s/m. If the energy dissipators were not installed, the movable weir openness height was lowered to create supercritical flow. In this case, a 0.5–3.9 m flow stabilization distance was found to be required. However, with the energy dissipators in place, hydraulic jump occurred in the movable weir downstream, shortening the flow stabilization distance to 0.4–0.8 m, approximately a 1/3 reduction from the non-installation case. Additionally, with the energy dissipator in place, the higher the movable weir openness heights were, the shorter the flow stabilization distance was.

If the movable weir openness heights were the same, the flow stabilization distances at 5% and 15% dissipator heights ranged from 0.4 to 1.9 m, which were similar to each other. However, the 15% installation height was found to have slightly higher numbers. The 10% dissipator installation height showed similar results to those of the 5% and 15% cases if the movable weir openness heights were at least 42 mm. However, if the movable weir openness heights were 39 mm or under, it showed smaller values by a maximum of 50% compared with the 5% and 15% height cases. The flow stabilization distance dependent upon energy dissipator installation heights was compared with the flow of the movable weir discharge. Figure 11 shows the flow stabilization distances after discharge according to Froude numbers.
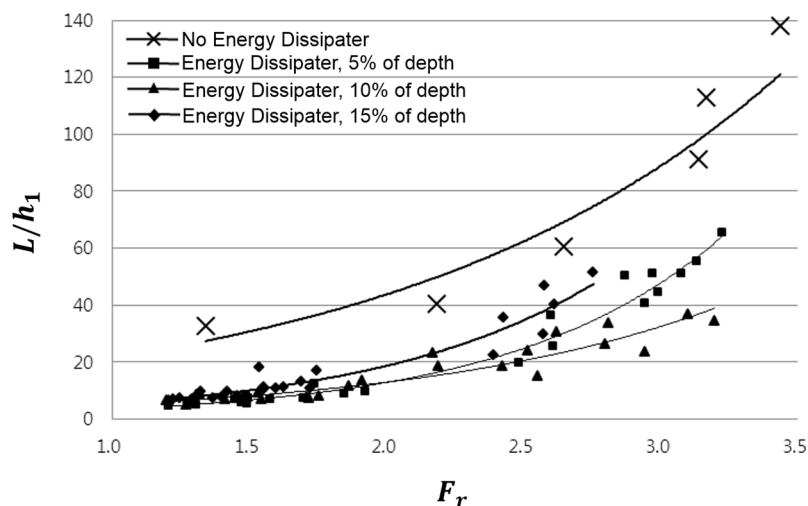

Figure 11. Length of flow stabilization after discharge from movable weir and Froude numbers.

If the energy dissipators were not installed, the Froude numbers of movable weir-discharged flow ranged from 1.342 to 3.437. The relation between the depth of supercritical flow and the length of flow stabilization (L/h_1) were from 30 to 137. With the dissipators in place, in a flow with a similar Froude number to that of the non-dissipator case, the dimensionless value of the length of flow stabilization divided by the depth of supercritical flow (L/h_1) was found to have a similar pattern according to Froude number. However, if the dissipators were installed, the dimensionless value of the length of flow stabilization (L/h_1) ranged from 4.68 to 65.52, showing approximately a 50% reduction.

If analyzed according to the energy dissipator installation heights, when the Froude numbers were 2.0 or under, the 5% height showed slightly more significant results than the other heights, but the energy dissipator heights were still not found to have a huge effect. However, if the Froude numbers exceeded 2.0, the 10% height showed that the dimensionless value of the length of flow stabilization (L/h_1) was shorter, and these gaps grew larger with Froude number increases. To examine energy dissipation according to energy dissipator installation, the energy at the discharge point in the movable weir (E_1) was compared with the energy in the stabilized flow after discharge (E_3).

Concerning the energy dissipation per unit length (($\Delta E/L$) according to dissipator heights, the 5% dissipator height showed per-length energy dissipation of 0.082 for every 1.0 Froude increase. The 10% height showed 0.126 and the 15% height showed 0.068, indicating the 5% and 15% heights had similar energy dissipation effectiveness. However, the 10% height was found to have at least 1.5 times greater energy reduction, as shown in Figure 12.

Regarding relative loss—the ratio of specific energy at the discharge point (E_1) and the specific energy reduced by the hydraulic jump (ΔE)—its calculation equation shown in Equation (4) and measurement results were reviewed. Table 5 expressed the relative energy loss measured by the experiment and calculated by theoretical principles as Equation (8) above. The relative energy loss in both the measured values and calculated values was found to tend to decrease as the Froude numbers decreased. This is because the weir upstream and downstream energy difference narrowed as the movable weir openness heights increased. In the present study, the measured values in the experiment were smaller than the theoretic values by 5%–10%, representing the gap between the experiment and theories.
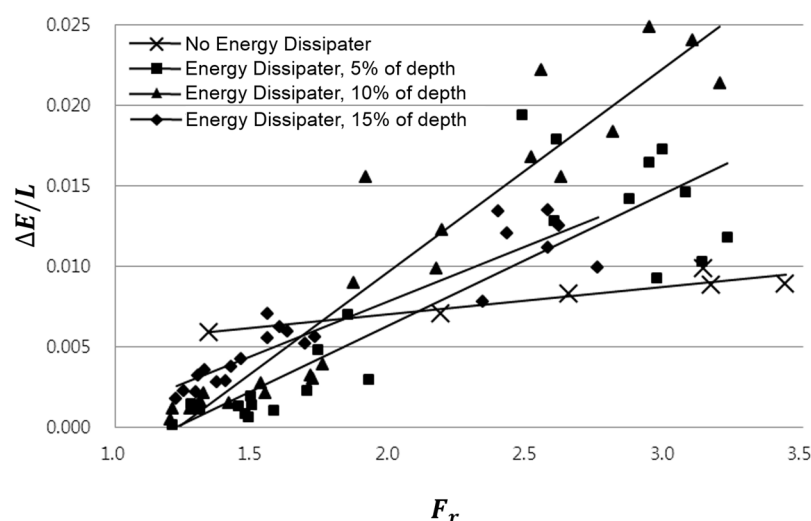

Figure 12. Energy dissipation per unit length according to dissipation block heights.

The energy after the end of hydraulic jump phenomenon was similar in most of the cases, as the downstream water level was fixed. However, at the same movable weir openness heights, the energy at the discharge point (E_1) was 135.44, 127.73 and 129.52 mm in the weir downstream at 5%, 10% and 15% heights, respectively, showing reduction. This is because the installed energy dissipators disturbed the flow discharged by the movable weir and reduced the cross-sectional area of flow to slow it down.

<center>**Table 5.** Relative energy loss (*q* = 0.052 m³/s/m).</center>

Height of Dissipator	Openness Height (m)	*Fr*	E_1	E_3	ΔE	Loss	
						Observed	Calculated
No issipator	0.036	3.43	153.60	118.93	34.67	23%	32%
	0.039	3.16	144.24	115.06	29.18	20%	28%
	0.042	3.14	144.94	117.29	27.65	19%	28%
5% of water depth	0.036	3.07	136.81	113.46	23.35	17%	27%
	0.039	2.99	139.77	115.58	24.19	17%	26%
	0.042	2.59	129.74	113.11	16.63	13%	19%
10% of water depth	0.036	2.81	131.91	111.72	20.20	15%	23%
	0.039	2.17	123.36	113.49	9.87	8%	12%
	0.042	2.51	127.92	112.80	15.12	12%	18%
15% of water depth	0.036	2.75	129.97	109.07	20.90	16%	22%
	0.039	2.58	130.16	110.13	20.03	15%	19%
	0.042	2.43	128.45	112.76	15.69	12%	16%

5.2. Energy Dissipation according to Energy Dissipator Installation Location

For energy dissipation, how to install energy dissipators was reviewed in this research. Two methods were reviewed regarding energy dissipator installation location and height. For each height, the installation locations were differentiated to examine the resulting changes. In the previous section on the changes in energy dissipator installation heights, three different heights were examined. For each of these heights, the dissipators were moved in four different locations 50%, 60%, 70% and 100% of downstream subcritical flow water depth (10 cm of this study) away from the movable weir. Figure 13 shows the increasing gaps in flow stabilization distances only according to Froude numbers both with and without energy dissipator installation cases and no significant change dependent upon dissipator installation locations.
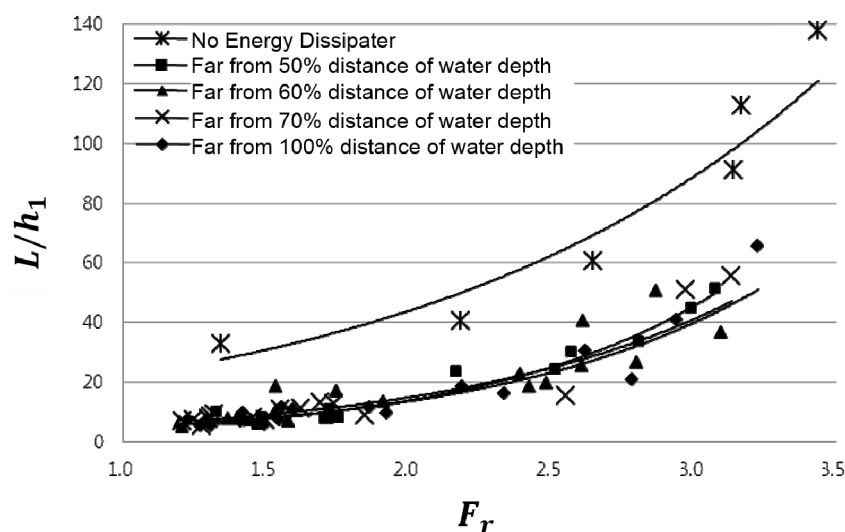
<center>**Figure 13.** Changes in water level and velocity according to dissipation block heights.</center>

6. Conclusion and Summary

In this study, a hydraulic experiment was performed by using a channel with a fixed weir and sluice gate-type movable weir installation to examine the resulting hydraulic jump and differences of each weir type. In the experiment, energy dissipator installation was considered to protect the bed under the movable weir. The following results were found:

Energy dissipators for energy reduction at the sluice gate were found to dissipate energy by more than 50% per unit length compared with the non-dissipator installation status if installed at a 10% height of the average river water depth in a location as far as approximately 70% of the average river water depth.

Although the sluice gate-type movable weir showed similar hydraulic jump lengths to those of the fixed weir, its supercritical flow length increased, so its length to the hydraulic jump start point rose considerably. For this reason, it is deemed that aprons for bed protection from scouring need to be 2–4 times sufficiently longer by considering the Froude numbers upon discharge.

Regarding hydraulic jump or the energy dissipation issues of sluice gate-type movable weirs, when movable-weir downstream water level differences grow larger or the discharge flow increases, their openness height should be elevated ($Fr < 2.5$) to protect the downstream area.

While fixed weirs involve drop head and flow diversion in dissipating energy, sluice gate-type movable weirs have no factor to help them dissipate energy other than the frictional force under the same upstream conditions and in the same discharge flow. Therefore, such movable weirs require apron installation of a sufficient length for frictional force-led energy dissipation.

In this study, a hydraulic experiment and numerical experiment were performed in a channel installed with a sluice gate-type movable weir to review hydraulic jump distances and hydraulic jump size changes. Thus, not only the hydraulic jump distances, but also the distances until hydraulic jump occurrence were researched. As sluice gate-type movable weirs create a supercritical flow region, they could cause hydraulic problems, including scouring in the bed due to flow velocity. In this case, it seems necessary to install energy dissipators.

To overcome the limitations of this hydraulic experiment, future hydraulic and numerical experiments are expected to involve more diverse conditions to propose a dissipation design for energy reduction and bed protection in the downstream of sluice gate-type movable weirs.

Author Contributions

Youngkyu Kim led the work performance; and Gyewoon Choi coordinated the research and contribution to writing the article; Hyoseon Park collected data through the experiment and review of papers; Seongjoon Byeon generated the result and wrote the manuscript.

Conflicts of Interest

The authors declare no conflict of interest.

References

1. Kim, Y.J. Energy Dissipation Effect of the Downstream at Under Flow Movable Weir. Ph.D. Thesis, Incheon National University, Incheon, Korea, 2013.
2. Sadati, S.K.; Speelman, S.; Sabouhi, M.; Gitizadeh, M.; Ghahraman, B. Optimal irrigation water allocation using a genetic algorithm under various weather conditions. *Water* **2014**, *6*, 3068–3084.
3. Michalec, B. The use of modified Annandale's method in the estimation of the sediment distribution in small reservoirs—A case study. *Water* **2014**, *6*, 2993–3011.
4. Peterka, A.J. *Hydraulic Design of Stilling Basins and Energy Dissipators*; A Water Resources Technical Publication Engineering Monography No. 25; United States Department of the Interior Bureau of Reclamation (USBR): Washington, DC, USA, 1964.
5. Bhowmik, G.N. *Hydraulic Jump Type Stilling Basins for Froude Number 2.5 to 4.5*; Report of Investigation 67; Illinois State Water Survey: Champaign-Urbana, IL, USA, 1971.
6. Rajaratnam, N.; MacDougall, R.K. Erosion by plane wall jets with minimum tailwater. *J. Hydraul. Eng. ASCE* **1983**, *109*, 1061–1064.
7. Yoon, S.; Lee, J.; Son, K.; Kim, J. Experiment study on downstream local scour of free-falling jet, *J. Korea Water Resour. Assoc.* **1995**, 28, 147–154. (In Korean)
8. Hoffmans, G.J.C.M.; Verheij, H.J. *Scour Manual*; A.A. Balkema: Rotterdam, The Netherlands, 1997; pp. 68–87.
9. Fahlbusch, F.E. Scour of rock due to the impact of plunging high velocity jets part I: A state-of-the-art review. *J. Hydraul. Res.* **2003**, *46*, 853–858.
10. Noshi, H.M. Energy dissipation near the bed downstream end sill. In Proceedings of of the 28th IAHR Congress, Graz, Austria, 22–27 August 1999; IAHR: Madrid, Spain; pp. 1–8.
11. Verma, D.; Goel, A. Development of efficient stilling basins for pipe outlets. *J. Irrig. Drain. Eng. Div.* **2003**, 126, 179–185.
12. Jung, J. Estimation of Apron Length Considering Weir Installation. Ph.D. Thesis, Incheon National University, Incheon, Korea, 2011.
13. Silvester, R. Hydraulic jump in all shapes of horizontal channels. *J. Hydraul. Div. ASCE* **1964**, *90*, 23–55.
14. Rajaratnam, N.; Subramanya, K. Profile of the hydraulic jump. *J. Hydraul. Div. ASCE* **1968**, *94*, 663–673.
15. Hager, W.H.; Bretz, N.V. Hydraulic jumps at positive and negative steps. *J. Hydraul. Res.* **1987**, *24*, 237–253.